NONLINEAR FLUID-STRUCTURE INTERACTION OF CLAMPED SHELLS

Kostas Karagiozis
Mechanical Science and Engineering, University of Illinois, Urbana, Illinois, U.S.A.
Michael P.Païdoussis, Arun K.Misra
Department of Mechanical Engineering, McGill University, Montreal, Quebec, Canada

ABSTRACT

The fluid structure interaction of shells and panels subjected to supersonic airflow has been investigated thoroughly in the past due to its importance in the aerospace industry. However, with advances in manufacturing, nuclear and biomedical engineering, there is a great need to further examine the nonlinear behaviour of shells in axial subsonic fluid flow. This paper describes an experimental and theoretical investigation of the nonlinear response of circular cylindrical shells subjected to axial fluid flow. The aim of this work was to gather important experimental data for (i) the critical flow velocity for instability, (ii) identifying the post-critical behaviour of the shell, and (iii) comparison with and validation of a new nonlinear theoretical model.

1. INTRODUCTION

For a long time, it was believed that subsonic/incompressible flows were associated with loss of stability in the form of mild divergence – in contrast to the vigorous flutter and richer dynamics observed with supersonic flows. However, new research in the early 1970s [Paidoussis and Denise (1972)] has sparked new interest in the analysis of shells subjected to subsonic flows. A full analytical linear model for cantilevered and clamped-clamped shells conveying incompressible fluid was provided, along with experimental results. In the clamped-clamped case, the experimental results showed that at sufficiently high flow velocity the system develops *flutter*. In contrast, the linear theoretical model predicts that the system loses stability by *divergence*, and then at higher flow velocity by coupled-mode flutter. The interval between the two is generally small, especially if the fluid conveyed is air. Hence, it was reasoned that in these experiments flutter was entrained by the divergence, and that was the reason why divergence was not observed. In the case of external (annular) flow, however, divergence *was* observed, but not flutter (though the maximum flow velocities available were probably insufficient for flutter). The interesting results described above for clamped-clamped shells (and also for cantilevered shells, not discussed here) have given the necessary impetus for the nonlinear analysis of shells containing, or immersed in, subsonic or incompressible flow. A new nonlinear analytical model was developed [see Amabili et al. (1999)] for shells with simply supported ends using the Donnell shallow shell nonlinear equations and the Païdoussis & Denise linear inviscid flow model for the fluid-structure interaction. This model predicted loss of stability by divergence and no oscillatory solutions. Similar results were obtained for external flow [see Amabili et al., 2001].

Mindful of the controversy on the existence of post-divergence coupled-mode flutter in pipes conveying fluid, only resolved via nonlinear theory [Païdoussis (2004)], it is clear that its existence for the shell problem must also be decided by nonlinear theory in this case – thereby clarifying also the nonexistence of divergence in the internal flow experiments.

The foregoing provide the motivation for performing new experiments and the development of a nonlinear theoretical model for shells with clamped ends to investigate the nonlinear behaviour of shells in axial flow.

2. THEORETICAL MODEL

The system under consideration is a thin circular cylindrical shell, of length L, mean radius R, and thickness h, as shown in Figure 1.

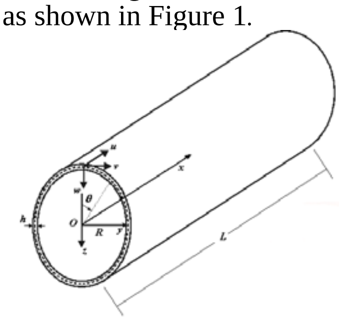

Figure 1: *Shell geometry and origin of coordinate system.*

The shell is assumed to be homogeneous and isotropic with Young's modulus E and Poisson ratio ν. A Cartesian coordinate system is assumed, with its origin attached at one end of the shell, denoting the middle surface displacements in the axial, circumferential and radial directions by *u*, *v*, and *w*, respectively.

2.1 Nonlinear structural model

The nonlinear Donnell theory for shallow shells is used to describe the large amplitude shell motion, assuming shell deformations to be dominated by the radial displacement *w*. In this formulation the effect of the in-plane inertia is assumed to be negligible. These theoretical approximations limit the applicability of the theory to shells with a minimum number of nodal diameters equal to 4 or 5; the circumferential wavenumber, *n*, is such that $1/n^2 \ll 1$ [see Donnell (1976)]. The equation of motion is

$$D\nabla^4 w + ch\dot{w} + \rho h\ddot{w} = -p + \frac{1}{R}\frac{\partial^2 F}{\partial x^2} + \left(\frac{\partial^2 F}{\partial y^2}\frac{\partial^2 w}{\partial x^2} - 2\frac{\partial^2 F}{\partial x\partial y}\frac{\partial^2 w}{\partial x\partial y} + \frac{\partial^2 F}{\partial x^2}\frac{\partial^2 w}{\partial y^2}\right), \qquad (1)$$

where *F* is the in-plane Airy stress function which satisfies the following compatibility equation:

$$\frac{1}{Eh}\nabla^4 F = -\frac{1}{R}\frac{\partial^2 w}{\partial x^2} - \frac{\partial^2 w}{\partial x^2}\frac{\partial^2 w}{\partial y^2} + \left(\frac{\partial^2 w}{\partial x\partial y}\right)^2; \qquad (2)$$

$D = Eh^3/\left[12\left(1-\nu^2\right)\right]$ is the flexural stiffness of the shell, ρ is its mass density, c $\left(\mathrm{kg/m^3 s}\right)$ the structural damping coefficient, and *p* the transmural pressure acting on the shell surface; $\nabla^4 = \left[\partial^2(\ )/\partial x^2 + \partial^2(\ )/\partial y^2\right]^2$, and the overdots represent time derivatives. Expressions for the relationships between stress resultants and shell displacements are given in Karagiozis et al. (2008).

In our analysis the clamped boundary conditions are used in the classical form given by

$$u = v = w = 0 \text{ and } \partial w/\partial x = 0 \text{ at } x=0 \text{ and } x=L. \qquad (3)$$

In order to reduce the continuous system to one of finite dimension, i.e. to discretize the system, the displacement *w* is expanded using an appropriate set of basis (shape) functions. Based on the work of Amabili et al. (1999) for simply supported shells, the following series expansion is proposed for the clamped-clamped shell model,

$$w(x,y,t) = \sum_{m=1}^{M}\sum_{n=1}^{N}\left[A_{m,n}(t)\cos(ny/R) + B_{m,n}(t)\sin(ny/R)\right]\varphi_m(x) + \sum_{m=1}^{K} A_{2m-1,0}(t)\varphi_{2m-1}(x), \qquad (4)$$

where φ_m are the eigenfunctions for a clamped-clamped beam defined by $\varphi_m(x) = \cosh(\lambda_m x/L) - \cos(\lambda_m x/L) - a_m\left[\sinh(\lambda_m x/L) - \sin(\lambda_m x/L)\right]$, λ_m being the corresponding dimensionless eigenvalues obtained from solving the characteristic equation $\cosh\lambda\cos\lambda = 1$; *m* is the axial wavenumber, *n* the circumferential wavenumber, and the coefficient $a_m = \left[\sinh\lambda_m - \sin\lambda_m\right]/\left[\cosh\lambda_m - \cos\lambda_m\right]$. The time functions $A_{m,n}(t)$, $B_{m,n}(t)$ and $A_{2m-1,0}(t)$ are the unknown generalized coordinates. The mode expansion given in Eq. (3) satisfies exactly the boundary conditions, and both the continuity of the circumferential displacement and the null in-plane displacement *v* at the shell ends [Karagiozis, 2006].

2.2 Fluid-structure interaction

In the case that fluid-structure interaction is present, the transmural pressure term, *p*, in the equation of shell motion (1) is non-zero. The shell is assumed to be in contact with an inviscid fluid, flowing in the axial direction. Furthermore, it is assumed that the fluid is incompressible and isentropic and the flow is irrotational. Nonlinearities in the dynamic pressure and in the boundary conditions at the fluid-structure interface are neglected, because fluid movements of the order of the shell thickness may be considered to be small; and hence a linear formulation is quite reasonable. [see Gonçalves and Batista (1988), Lakis and Laveau (1991), and Selmane and Lakis (1997)]. In addition, pre-stress in the shell due to fluid weight (hydrostatic effect) is neglected. With these assumptions, the fluid structure-interaction can be described by potential flow theory. The potential flow is comprised of two terms; one which is represented by the uniform undisturbed axial mean flow velocity, and the other one by the unsteady flow. The expression for the unsteady potential flow is obtained by solving the Laplace equation

$$\nabla^2\Phi = \frac{\partial^2\Phi}{\partial x^2} + \frac{\partial^2\Phi}{\partial r^2} + \frac{1}{r}\frac{\partial\Phi}{\partial r} + \frac{1}{r^2}\frac{\partial^2\Phi}{\partial\theta^2} = 0, \qquad (5)$$

where $\Phi(x,\theta,r,t)$ is the unsteady potential flow, *r* is the radial coordinate, and $\theta = y/R$. Accordingly, the total perturbed pressure *P* acting on the fluid-shell interface is defined as the combination of the mean pressure $\overline{P}$ and the perturbation pressure p, i.e., $P = \overline{P} + p$. The perturbation pressure is found using the linearized Bernoulli equation yielding

$$p = -\rho_F\left(\partial\Phi/\partial t + U\,\partial\Phi/\partial x\right). \qquad (6)$$

Furthermore, the fluid is assumed to be a cylinder of infinite length, which lies within a periodically supported shell of infinite length. This assumption allows us to use the method of separation of variables in the solution of the velocity potential. This requires an expression for *w* that satisfies the essential boundary conditions exactly for

$0 \le x \le 2L$. This expansion for w is substituted into equation (5) and the solution for Φ is obtained using the separation of variables method. In the radial direction the two boundary conditions used are:

$$r = 0 \Rightarrow \text{ finite flow}, \; r = R \Rightarrow \frac{\partial \Phi}{\partial r} = \left(\frac{\partial w}{\partial t} + U \frac{\partial w}{\partial x} \right), \quad (8)$$

where the second is the impermeability condition.

To ensure compatibility between the flow solution and the modal expansion for the shell displacements, a new relationship must be established for the solution of the velocity potential in the axial direction and the eigenfunctions involved in the solution expansion given in Eq.(4) [for details see Karagiozis (2008, 2006)]. This compatibility condition imposes a transformation of the clamped beam eigenfunctions to a series involving sine functions of the same wavelength. Therefore, the general form of the solution for w is given by

$$w(x,\theta,t) = \sum_{m=1}^{M} \sum_{n=0}^{N} w_{m,n}(x,\theta,t)$$

$$= \sum_{m=1}^{M} \sum_{n=0}^{N} \sum_{j=1}^{KK} b_{m,j} \sin(j\pi x/L) \left[A_{m,n}(t) \cos(n\theta) + B_{m,n}(t) \sin(n\theta) \right], \quad (9)$$

where M, N *and* KK are integers, $\theta = y/R$, and

$$b_{m,j} = \frac{2}{L} \sum_{j=1}^{KK} \int_0^L \varphi_m(x) \sin(j\pi x/L) \, \mathrm{d}x, \quad (10)$$

in which $\varphi_m(x)$ appeared in Eq. (4).

Using Eq. (9) and the radial boundary conditions for the fluid, given in Eq. (8) the solution for the perturbation velocity potential is

$$\Phi = -\sum_{m=1}^{\infty} \sum_{n=0}^{\infty} \sum_{j=1}^{\infty} \frac{\mathrm{I}_n(k_m r)}{\mathrm{I}_n'(k_m r)\big|_{r=R}} \left[\cos(n\theta) + \sin(n\theta) \right]$$

$$\times \left[b_{m,j} \sin(m\pi x/L) \dot{\zeta}_{m,n}(t) + U b_{m,j} (m\pi/L) \cos(m\pi x/L) \zeta_{m,n}(t) \right], \quad (11)$$

where the prime denotes differentiation with respect to r and the overdot indicates differentiation with respect to t. The final expression for the perturbation pressure is found by using the solution of the velocity potential in Eq.(11) into Eq. (6).

Expressions for the perturbation pressure of the annular fluid can be derived in a similar fashion.

3. EXPERIMENTS

Four different experimental set-ups were employed to investigate the stability of shells of different materials and with different flow configurations. The first set of experiments was conducted with elastomer shells and annular air-flow. The second was with elastomer shells and internal air-flow. The third and fourth sets were, respectively, with aluminium and plastic polyethylene terephthalate (PET) shells and internal water flow. The experimental apparatuses and procedures are discussed in detail in Karagiozis et al. (2005) and shall not be presented here.

The elastomer shells used were made of silastic (RTV silicone rubber) [see Païdoussis (1998, Appendix D)]. The average values of the material properties are given in Table 1. Here E is Young's modulus, ρ the mass density of the shell, and ν the Poisson ratio.

Properties	$E\left[\mathrm{N/m^2}\right]$ (psi)	$\rho\left[\mathrm{kg/m^3}\right]$ $(\mathrm{lb/ft^3})$	ν
Elastomer	2.82×10^5 (40.9)	1.16×10^3 (7.2×10)	0.47
Aluminium	70×10^9 (10×10^6)	2.7×10^3 (1.70×10^2)	0.33
PET	2.3×10^9 (3.3×10^6)	0.8×10^3 (5.0×10)	0.4

Table 1: Shell material properties

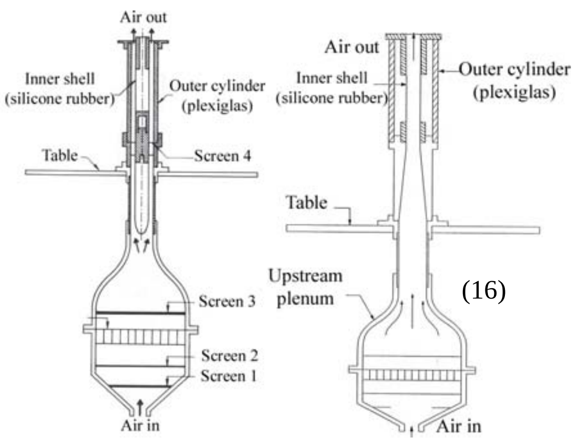

(a) (b)

Figure 2: *Set-up for (a) annular and (b) internal air-flow experiments.*

Figure 2 shows the two variants of the apparatuses used in the elastomer shell – air experiments. In the third and fourth sets of experiments the aluminium or PET shell is mounted vertically in the plexiglas test-section of a water tunnel. The space between the outer surface of the shell and the test-section is filled with quiescent water, which could be pressurized, if desired, via an external pressure line. Figure 3 shows the apparatus used in the aluminium/PET internal water-flow experiments.

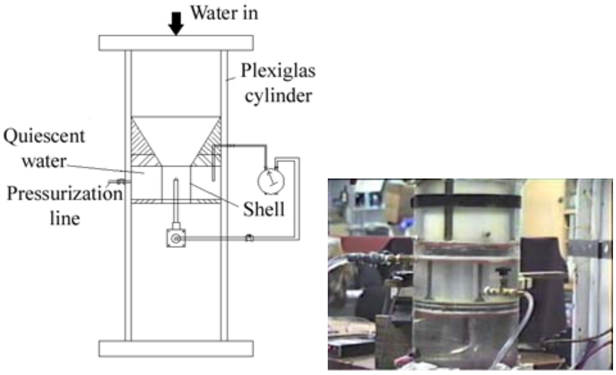

Figure 3: *Apparatus for water tunnel experiments.*

The shell dimensions used in the annular elastomer air-flow and the internal aluminium/PET water-flow experiments are listed in Table 2.

Properties	Length [mm], (in)	Thickness [mm], (in)	Length/radius *L/R*
Elastomer Annular	40 (1.57)	1.5 (0.059)	1.7
Elastomer Internal	75 (2.95)	1.5 (0.059)	3
Aluminium	122.5 (4.82)	0.137 (0.005)	2.98
PET	100.1 (4.94)	0.3 (0.012)	2.41

Table 2: Shell dimensions

A comparison of experimental observations and results with numerical results obtained from the nonlinear model described above is described next.

4. COMPARISON OF EXPERIMENTAL AND THEORETICAL RESULTS

The partial differential equation of motion was discretized to a set of second-order ordinary differential equations via a Galerkin technique. These equations are transformed into two first-order equations and studied using the software AUTO 97 (Doedel et al., 1998) for continuation and bifurcation analysis of nonlinear ordinary differential equations.

For the theoretical results presented in this paper the following nondimensionalizetion for the flow velocity is used:

$$V = U \Big/ \left\{ \left(\pi^2 / L \right) \left(D / (\rho h) \right)^{1/2} \right\}. \qquad (12)$$

4.1 Annular-air experiments

A comparison of the theoretical versus the experimental results for the elastomer shell subjected to annular air-flow and n=4 is shown in Figure 4. This is a bifurcation diagram of the nondimensional shell amplitude at $x = L/2$ versus the nondimensional air-flow velocity, V. The theoretical results shown were obtained using an extended eleven degree-of-freedom model. The transmural pressure was set to $\Delta P_{tm}\left(L/2\right) = 0$ in this case, although in reality there is a small transmural pressure present in the experiments.

Both theoretical and experimental results indicate loss of stability by divergence, and no oscillatory motions in the velocity range considered. In addition, the theoretical results predict a large hysteresis between the onset of divergence and the folding point (the point at which unstable Branch 2 becomes stable), characterizing a subcritical post-buckling behaviour of the clamped elastomer shell; the same kind of hysteresis was observed in the experiments.

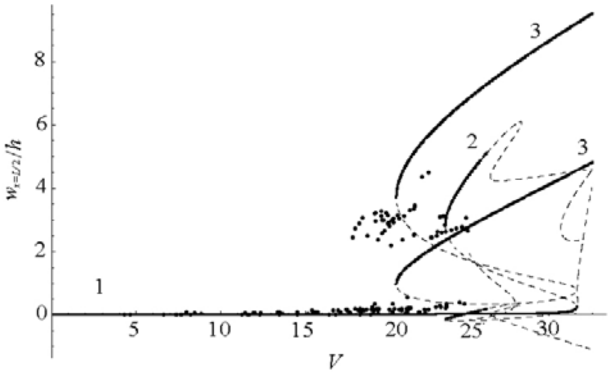

Figure 4: *Elastomer shells and annular air-flow results:* ——— *, stable solutions,* – – – – *, unstable solutions; ●, experimental data points.*

4.2 Internal-air experiments

In all internal air-flow cases the shell system lost stability by divergence leading to oscillatory or "*dynamic*" divergence. The mechanism of dynamic divergence is discussed in detail in Karagiozis et al. (2005); briefly, it is as follows: (i) the shell loses stability by static divergence; but, due to the large flexibility of the elastomer shell, the deformation is large enough (in many cases reducing the flow area by 50% or more), to cause a pressure build-up upstream of the shell; (ii) this pressure build-up causes the shell to open up and to buckle in the antiphase shape; (iii) this phenomenon is repeated again and again, giving the impression of an oscillatory instability. Fig. 5(a) shows in a series of photographs the dynamic buckling phenomenon, as observed for a shell with *L/R*=3 with n=4.

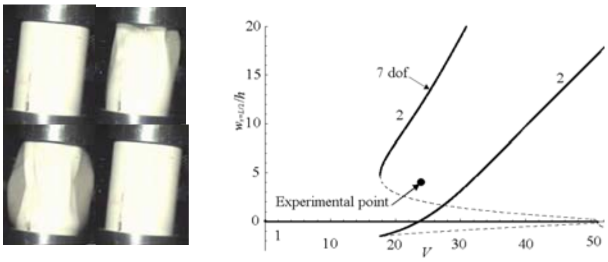

(a) (b)

Figure 5: *Nonlinear response of elastomer shells in internal air-flow: (a) snapshots of dynamic divergence response for L/R=3; (c) comparison of experiments and theory for L/R=4.4.*

In Fig 5(b), the theoretical results indicate loss of stability by divergence with a large subcritical bifurcation. In Karagiozis (2006), it was concluded that very pliable shells lose stability by divergence, giving rise to this dynamic buckling phenomenon, because of the large flow-constricting shell deformation involved. It is believed that Païdoussis and Denise (1973) observed the same phenomenon in their experiments but misinterpreted it as flutter; [see Païdoussis (2004)].

4.3 Internal-water experiments

A typical set of experimental and theoretical results for an aluminium shell subjected to internal water flow, a transmural pressure of 5.80 kPa and n=6 is shown in Figure 6.

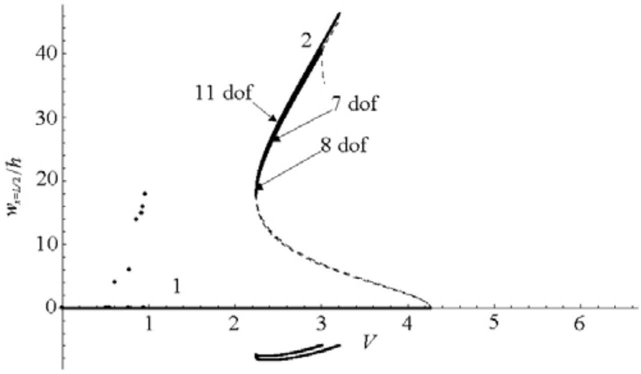

Figure 6: *Aluminium shell and internal water flow for* $\Delta P_{tm}(L/2) = 5.8$ kPa *; ——, stable solutions; – – – –, unstable theoretical solutions; ●, experimental data points.*

Both experiment and theory indicate that the shell lost stability by divergence exhibiting a strong subcritical bifurcation with a large hysteresis. However, quantitatively, the theoretical results are not close to the experimental data points. The reason for this disagreement lies on the nature of the boundary conditions in the experiments. In Karagiozis et. al. (2006) it is shown that the experimental boundary conditions for this experiment were simulating a boundary condition intermediate between clamped and simple supports. Nevertheless, no oscillatory solutions were obtained in either the experiment or theory.

Figure 7(a) shows results of a PET and internal water flow. Both experimental and theoretical results are in excellent agreement predicting loss of stability by divergence following a large hysteretic subcritical bifurcation with n=6. In Figure 7(b) additional numerical experiments indicated that for specific values of the transmural pressure there is a range of flow velocities in which dynamical shell responses are predicted that lead to periodic, quasi-periodic and chaotic shell oscillations, as discussed in Karagiozis et al. (2007).

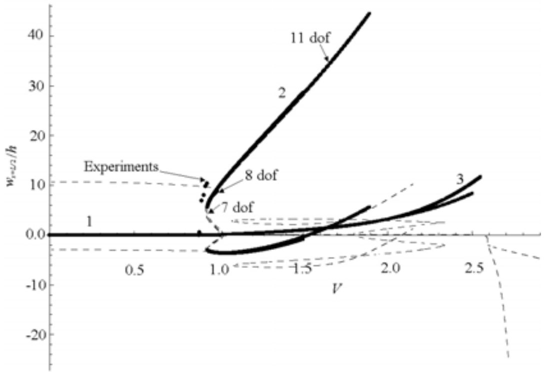

(a)

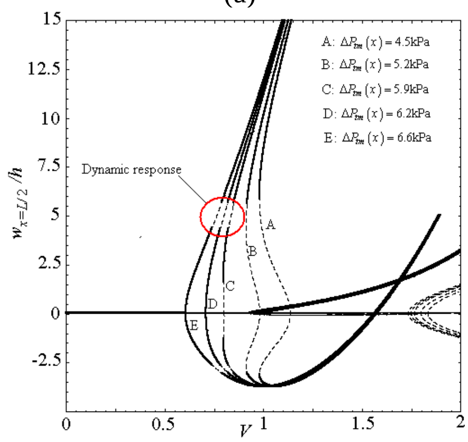

(b)

Figure 7: *Clamped PET subjected to internal water flow: (a) comparison of experimental and theoretical results; (b) numerical results showing dynamical regions of chaotic oscillations for different transmural pressure values.*

5. CONCLUSION

Typical theoretical and experimental results are presented indicating loss of stability by static, strongly subcritical divergence. No post-divergence dynamic instabilities or other oscillatory solutions were found to exist, except in small flow-windows for cases with considerable transmural pressure.

The model found multiple solutions for specific values of the flow velocity, indicating that a jump from one stable solution to another is possible if enough perturbation is given to the shell system.

In the experiments in Figs. 4, 6, and 7, it was found that the system lost stability by static divergence (buckling). Moreover, a strong hysteresis between the onset and, as the flow velocity was decreased, the cessation of divergence was found. Both these findings are in full qualitative agreement with the predictions of the theoretical model of a strongly subcritical static divergence. In the case of elastomer shells conveying air-flow, Fig. 5(a), the shell was observed to lose stability dynamically with very large amplitudes. However, as reasoned in Païdoussis (2003) and Karagiozis et al. (2005), what appears as an oscillatory instability is in fact a dynamic divergence phenomenon, associated with the flow constriction resulting from the large amplitudes of divergence in such pliable shells. Significantly, with the stiffer aluminium and PET shells, the system lost stability by static divergence, in agreement with the theoretical model.

In general, the theoretical models predicted with excellent accuracy the qualitative changes in shell behaviour, and with reasonably good or excellent quantitative agreement the critical and post-divergence behaviour of the experimental systems investigated. From the design point of view, this study shows that the critical flow velocity for shells cannot be predicted by a linear analysis, and that existing safety criteria may be inadequate, due to the subcritical bifurcation associated with loss of stability.

6. ACKNOWLEGMENTS

The authors would like to thank NSERC of Canada and FQRNT of Québec for their financial support.

7. REFERENCES

Amabili, M., Pellicano, F., M.P.Païdoussis, 1999, Nonlinear dynamics and stability of circular cylindrical shells containing flowing fluid. Part I: Stability. *Journal of Sound and Vibration* **225**: 655-699.

Amabili, M., Pellicano, F. and Païdoussis, M.P., 2001, Nonlinear stability of circular cylindrical shells in annular and unbounded axial flow. *Journal of Applied Mechanics*, **68**: 827-834.

Doedel, E.J., Champneys, A.R., Fairgrieve, T.F., Kuznetsov, Y.A., Sandstede, B., Wang, X., 1998, *AUTO 97: Continuation and Bifurcation Software for Ordinary Differential Equations* (with HomCont), Concordia University, Canada.

Donnell, L.H., 1976, *Beams, Plates and Shells*, McGraw-Hill, New York.

Gonçalves, P.B., Batista, R.C., 1988, Non-linear vibration analysis of fluid-filled cylindrical shells. *Journal of Sound and Vibration* **127**: 133-143.

Karagiozis, K.N., 2006, Experiments and theory on the nonlinear dynamics and stability of clamped shells subjected to axial fluid flow or harmonic excitation, Ph.D. Thesis, McGill University.

Karagiozis, K.N., Païdoussis, M.P., Misra, A.K., Grinevich, E., 2005, An experimental study of the nonlinear dynamics of cylindrical shells with clamped ends subjected to axial flow. *Journal of Fluids and Structures* **20**: 801-816.

Karagiozis,K.N., Païdoussis, M.P., Misra, A.K., 2007, Transmural pressure effects on the stability of clamped cylindrical shells subjected to internal fluid flow: Theory and experiments *International Journal of Non-Linear Mechanics* **42**: 13-23.

Karagiozis,K.N., Païdoussis, M.P., Amabili,M., Misra, A.K., 2008, Nonlinear stability of cylindrical shells subjected to axial flow: Theory and experiments. *Journal of Sound and Vibration*, **309**: 637-676.

Lakis, A.A., Laveau, A., 1991, Non-linear dynamic analysis of anisotropic cylindrical shells containing a flowing fluid. *International Journal of Solids and Structures* **28**: 1079-1094.

Païdoussis, M.P., 1998, *Fluid Structure Interaction: Slender Structures and Axial Flow*, Vol. 1, London: Academic Press.

Païdoussis, M.P., 2004, *Fluid-Structure Interactions: Slender Structures and Axial Flow*, Vol. 2, Elsevier Academic Press, London, UK.

Païdoussis, M.P., Denise, J.P., 1972, Flutter of thin cylindrical shells conveying fluid. *Journal of Sound and Vibration* **20**: 9-26.

Selmane, A, Lakis, A.A., 1997, Non-linear dynamic analysis of orthotropic open cylindrical shells subjected to a flowing fluid. *Journal of Sound and Vibration* **202**: 67-93.